Progress In Electromagnetics Research C, Vol. 87, 73–85, 2018

A New Synthesis Algorithm for Minimization of Coplanar Distributed Antenna Arrays in WSNs

Heba S. Dawood, Amr H. Hussein*, Entesar Gemeay, and Mahmoud A. Attia

Abstract—Distributed antenna arrays are arbitrarily large groups of neighboring nodes which are controlled to form virtual antenna arrays for both transmission and reception. Distributed beamforming (DBF) is widely used in wireless sensor networks (WSNs) and distributed massive Multi-Input Multi-Output (MIMO) systems. The research in DBF has been divided into four major research trends: radiation pattern analysis, optimization of power and lifetime, nodes synchronization, and array design. In this paper, a new algorithm is introduced to synthesize the radiation pattern of an arbitrarily distributed array using reduced number of distributed nodes. In this context, the reduction in the number of nodes results in minimizing the synchronization complexity between the synthesized array nodes and in minimizing the number of RF front ends. Thus, the overall system cost is reduced. In this algorithm, the three antenna array parameters (number of nodes, nodes locations, and nodes excitation) are properly adjusted to construct a close copy of the original array pattern. Different nodes selection ways are utilized to select the nodes required to synthesize the array for a desired radiation pattern. Also, uniform feeding and non-uniform feeding scenarios are introduced. In simulations, the proposed algorithm is applied to the synthesis of pencil-beam patterns. The simulation results reveal that the synthesized radiation patterns highly agree with the ordinary distributed array pattern in the case of non-uniform feeding. Also, the proposed algorithm can be applied to the synthesis of shaped-beam patterns via controlling the three aforementioned antenna array parameters and taking the shaped-beam pattern as the desired pattern in the algorithm.

1. INTRODUCTION

Wireless Sensor Networks (WSNs) are composed of sensor nodes distributed in a specific area. The nodes are small devices which cooperate for sensing, collecting and processing information. Energy efficiency is an important issue in WSNs as sensor nodes have a limited power supply [1, 2]. The nodes of WSN can be distributed in different bound areas such as circle, sphere, and triangle [3, 4]. They are combined to form a distributed antenna array. Traditionally, the antenna array consists of a periodic structure of antenna elements. However, the periodic arrays have some problems such as scan blindness and tight fabrication constraints [5]. The randomness of distributed nodes mitigates these problems and also increases the bandwidth of the pattern. The distributed beamforming (DBF) is an effective solution for increasing communication range and saving transmission energy in WSNs. Also, it is suitable for 5G communications, massive MIMO, and machine-to-machine (M2M) communications [6–8]. It combines the radiation from each node to generate a directive pattern towards the intended receiver. However, the randomness of the distributed nodes causes observable variations in the pattern. Also, the side lobes are affected in both amplitude and position by the WSN topology. And it is worth noting that the side lobe levels resulting from randomly distributed arrays are higher than that of the traditional

Received 11 June 2018, Accepted 16 August 2018, Scheduled 22 September 2018

* Corresponding author: Amr Hussein Hussein Abdullah (amrvips@yahoo.com).
The authors are with the Electronics and Electrical Communications Engineering Department, Faculty of Engineering, Tanta University, Tanta, Egypt.

antenna arrays, especially when the number of distributed nodes is small. The high side lobe level acts as interference for unintended receivers located within the same range [9–12]. So, it is important to make a compromise between the number of nodes in WSN and the produced side lobe level (SLL).

Many research efforts to synthesize pencil-beam linear antenna arrays are exerted such as the matrix pencil method (MPM) [13] and the forward-backward matrix pencil method (FBMPM) [14]. On the other hand, the synthesis of shaped-beam linear antenna arrays has a valuable effect in wireless communications. In [15], an algorithm based on a hybrid combination between the Method of Moments (MOM) and the Genetic Algorithm (GA) is introduced for the synthesis of both pencil-beam and shaped-beam linear antenna arrays. In [16], a powerful approach for power synthesis of linear antenna arrays radiating shaped-beams lying in an arbitrary mask is introduced. The approach is based on linear programming optimization and polynomial factorization to deal with the case where antenna elements excitations must have even distribution.

In this paper, a new distributed beamforming algorithm is introduced to synthesize arbitrarily distributed pencil-beam antenna arrays using reduced number of nodes in Wireless Sensor Networks. A replica of the ordinary array pattern is produced via controlling the number of nodes, nodes locations, and excitations in a well-defined circular bound area. The produced patterns are synthesized using uniform feeding and non-uniform feeding. Also, the proposed algorithm can be applied to the synthesis of shaped-beam patterns by taking the intended shaped-beam pattern as the desired pattern in the algorithm. The paper is organized as follows. In Section 2, the proposed distributed array synthesis algorithm is presented in details. The simulation results are shown in Section 3, and the conclusion is given in Section 4.

2. PROPOSED DISTRIBUTED ARRAY SYNTHESIS ALGORITHM

The distributed beamforming is widely used in distributed antenna arrays to achieve energy efficiency in long distance transmission. However, as the number of distributed nodes increases, the cost of the RF front end chains increases, and the complexity of nodes synchronization increases. From this point of view, a new distributed array synthesis algorithm is introduced to construct a close replica of the array pattern using fewer nodes. In this algorithm, the three antenna array parameters (number of nodes, nodes locations, and nodes excitations) are properly adjusted. The proposed algorithm is clearly described in the following sections of the paper.

2.1. System Model

Consider K nodes which are distributed over a disk with a radius R meter. Each kth node has a polar coordinates (r_k, ψ_k) where r_k is the distance of node k from the central point, $r_k \in [0, R]$, and ψ_k is the azimuth angle of node k from the central point or cluster head (CH), $\psi_k \in [-\pi, \pi]$. Some assumptions are made in this paper for simplicity. These assumptions are commonly made in [8–11]. It is assumed that all nodes are isotropic antennas and coplanar with each other. Furthermore, all nodes are perfectly synchronized in phase, time, and frequency. Also, consider an intended receiver with spherical coordinates location (A, θ_0, φ_0), where A is the distance between the intended receiver and central point, θ_0 the elevation direction $\theta_0 \in [0, \pi]$, and φ_0 the azimuth direction, $\varphi_0 \in [-\pi, \pi]$. Also, assume that the intended receiver is within the same plane as the distributed nodes where $\theta_0 = \frac{\pi}{2}$. The geometrical configuration of the distributed antenna array is illustrated in Fig. 1.

2.2. Steps of the Proposed Distributed Array Synthesis Algorithm

2.2.1.

The ordinary array pattern of K distributed nodes with coordinates $r = [r_1, r_2, \ldots, r_K]$ and $\psi = [\psi_1, \psi_2, \ldots, \psi_K]$ is expressed as follows [8];

$$AF(\varphi) = \frac{1}{K} \sum\nolimits_{k=1}^{K} w_k e^{j \frac{2\pi}{\lambda} d_k(\varphi)} \tag{1}$$

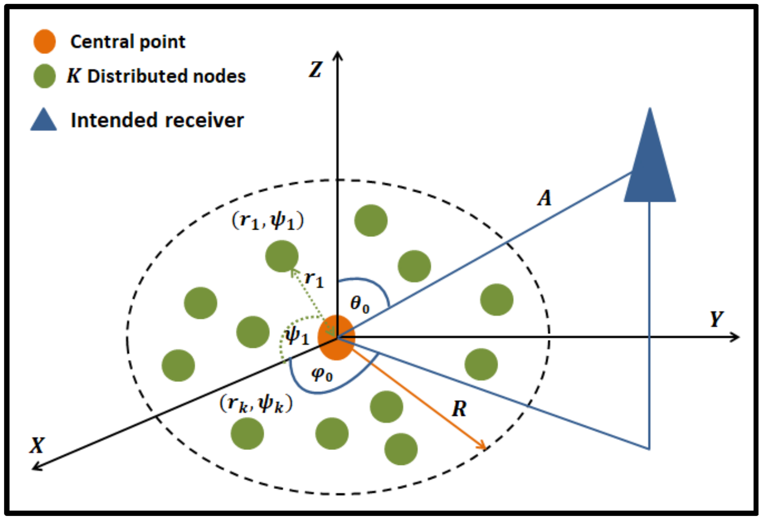

Figure 1. The geometrical configuration of distributed antenna array.

where $d_k(\varphi)$ is the Euclidean distance between the kth node and the far filed point. $d_k(\varphi)$ is calculated according to Eq. (2) [8];

$$d_k(\varphi) = A - r_k \cos(\varphi - \psi_k) \tag{2}$$

where w_k is the kth node transmission weight which is calculated as follows;

$$w_k = \xi_k e^{j\Psi_k} \tag{3}$$

where ξ_k and Ψ_k are the kth node transmission energy and the initial transmission phase, respectively. $\xi_k = 1$, and Ψ_k is determined as follows;

$$\Psi_k = -\frac{2\pi}{\lambda} d_k(\varphi_0) \tag{4}$$

where $d_k(\varphi_0)$ is the Euclidean distance between the kth node and the intended receiver. The ordinary array pattern has a main beam towards the direction of the intended receiver φ_0. To synthesize the array pattern with reduced number of nodes, Eq. (1) is rewritten as follows;

$$AF_{syn}(\varphi) = \frac{1}{M} \sum\nolimits_{m=1}^{M} v_m e^{j\frac{2\pi}{\lambda} d_m(\varphi)} \tag{5}$$

where $AF_{syn}(\varphi)$ is the synthesized array pattern, M the new number of distributed nodes such that $M < K$, and v_m is the synthesized transmission weight of the mth node which is calculated as follows;

$$v_m = \delta_m e^{j\Psi_m} \tag{6}$$

where δ_m is the synthesized transmission energy of the mth node, and Ψ_m is the initial transmission phase of the mth node which is obtained according to Eq. (3).

Taking $AF(\varphi)$ as the desired array pattern, $AF_d(\varphi)$, which is needed to be synthesized with reduced number of distributed nodes. $AF(\varphi)$ may be pencil-beam pattern or shaped-beam pattern.

$$AF(\varphi) = AF_d(\varphi) \tag{7}$$

Substituting by $AF_d(\varphi)$ and v_m in Eq. (5);

$$AF_{syn}(\varphi) = \frac{1}{M} \sum\nolimits_{m=1}^{M} \delta_m e^{j\Psi_m} e^{j\frac{2\pi}{\lambda} d_m(\varphi)} = AF_d(\varphi) \tag{8}$$

Eq. (8) can be transformed into the matrix form as follows;

$$\frac{1}{M} \times [\delta]_{1\times M} \times [Q]_{M\times N} = [O]_{1\times N} \tag{9}$$

where N is the number of samples of the desired array patter. $Q(M \times N)$ is the matrix which contains the samples of $e^{j\Psi_m} e^{j\frac{2\pi}{\lambda} d_m(\varphi)}$ for $\varphi = [\varphi_1, \varphi_2, \ldots, \varphi_N]$. δ is the $(1 \times M)$ vector representing synthesized energy transmission of the distributed nodes where $\delta = [\delta_1, \delta_2, \ldots, \delta_M]$. O is a $(1 \times N)$ vector which contains the samples of the desired array pattern for $\varphi = [\varphi_1, \varphi_2, \ldots, \varphi_N]$.

2.2.2. Number of Distributed Nodes Selection

In the deterministic linear and planner antenna arrays, the array size is related to the number of nodes and nodes spacing. In order to get a replica of a radiation patter, the synthesized and original arrays should have the same array size, so that the minimum number of nodes required to synthesize the array pattern can be easily determined [15]. However in distributed arrays, the randomness of nodes makes it difficult to estimate the minimum number of node. So for a given number of nodes $M < K$ distributed over the same disk radius R, the algorithm is executed.

2.2.3. Nodes Locations Selection

In this step, three different schemes to select the locations of the desired number of nodes M are described as follow;

a. The desired M nodes are selected sequentially from the original distributed K nodes with the same locations such that

$$(r_m, \psi_m) = (r_k, \psi_k), \quad m = k = 1, 2, \ldots, M \tag{10}$$

b. The desired M nodes are selected randomly from the original distributed K nodes with the same locations such that

$$(r_m, \psi_m) = (r_k, \psi_k), \quad m = 1, 2, \ldots, M \text{ and } m \neq k \text{ or } m = k \tag{11}$$

c. The desired M nodes are distributed randomly over the same disk with radius R with new locations where

$$(r_m, \psi_m) \neq (r_k, \psi_k), \quad m = 1, 2, \ldots, M \tag{12}$$

2.2.4.

From step 3, after the knowledge of M and the corresponding locations (r_m, ψ_m), the synthesized energy transmission of the mth node can be obtained by solving Eq. (9) as follows;

$$\delta = M \cdot (O/Q) \tag{13}$$

Once the nodes energy transmissions are updated, the synthesized array pattern $AF_{syn}(\varphi)$ is constructed with the main beam directed towards the intended receiver direction φ_0. The synthesized and original patterns have nearly identical main beams, but with minor changes in the side lobes.

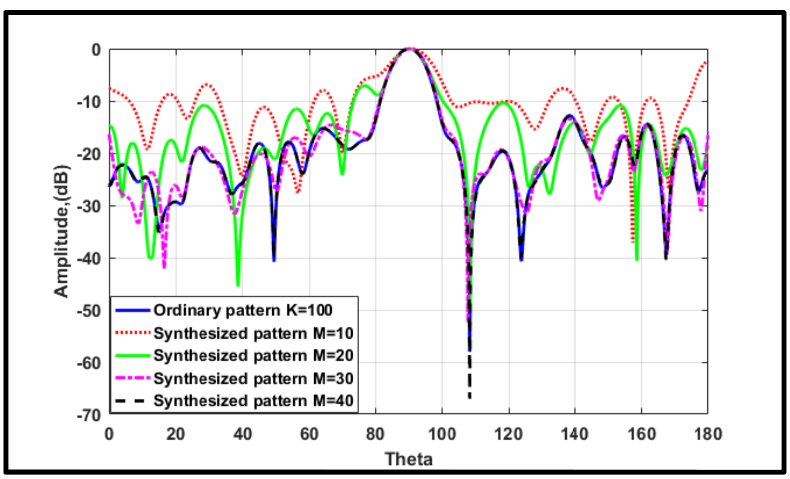

Figure 2. The synthesized patterns using non-uniform feeding for $M = 10$, 20, 30, and 40 compared to the ordinary pattern using $K = 100$ for case (a) of nodes locations selection.

3. SIMULATION RESULTS

In this section, the three different location selection schemes of the desired number of M nodes are carried out to stand up in the best way to select the reduced number of distributed nodes in order to construct the synthesized pattern. The comparisons between these scenarios are made in terms of the mean square error (MSE) between the desired and synthesized patterns according to Eq. (14);

$$\mathrm{MSE} = \frac{1}{N}\sum\nolimits_{n=1}^{N} \left[\left\|AF_{syn}(n) - AF_{d}(n)\right\|\right]^2 \tag{14}$$

In all scenarios, consider a $K = 100$ distributed pencil-beam antenna array whose nodes are randomly distributed over a circular disk area of radius $R = 6\,\mathrm{m}$. Also, consider that the direction of the intended receiver is at $\varphi_0 = 90°$. The goal of all scenarios is to estimate the synthesized pattern using a reduced

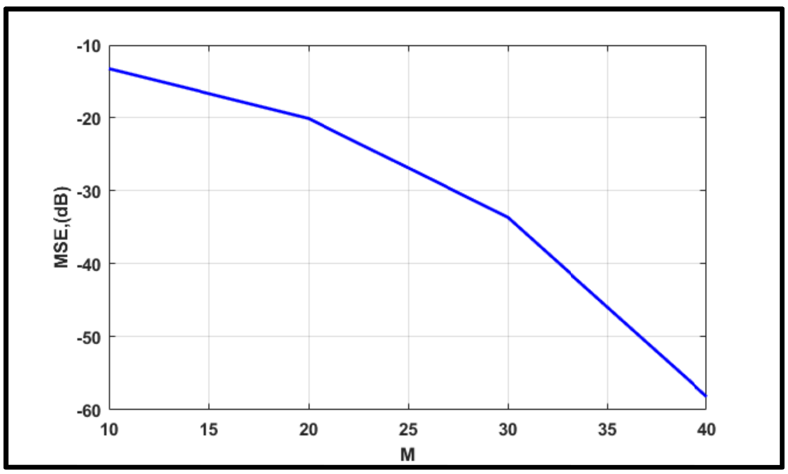

Figure 3. The MSE versus the number of nodes M for synthesized patterns using non-uniform feeding for case (a) of nodes locations selection.

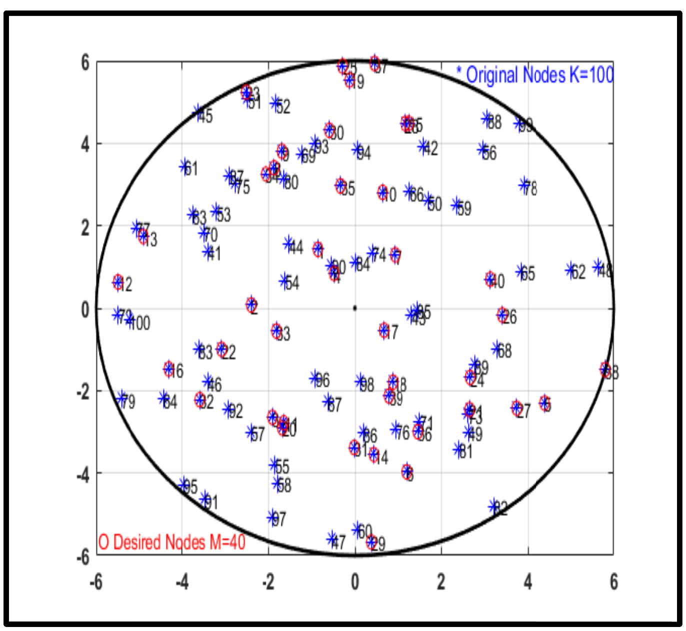

Figure 4. The distribution of $M = 40$ and $K = 100$ nodes over $R = 6\,\mathrm{m}$ for case (a) of nodes locations selection.

number of distributed nodes $M < K$ with minimum MSE. Furthermore, the proposed algorithm is executed for different numbers of nodes $M = 10$, 20, 30, and 40 to select the smallest M which provides a synthesized pattern with minor variations from the ordinary pattern.

Scenario (1): In this scenario, the desired M nodes are selected sequentially from the original distributed K nodes with the same polar coordinates according to Eq. (10). The synthesized patterns using non-uniform feeding for $M = 10$, 20, 30, and 40 are shown in Fig. 2. It is clear that the synthesized pattern using $M = 40$ coincides with the ordinary pattern using $K = 100$. The MSE versus the number of nodes M of the synthesized patterns is shown in Fig. 3. The MSEs for $M = 10$, 20, 30, and 40 are -13.2336 dB, -20.0579 dB, -33.587 dB, and -58.1917 dB, respectively. Fig. 4 shows the distribution of the selected $M = 40$ nodes and the original $K = 100$ nodes. On the other hand, for $M = 40$, the corresponding synthesized pattern using uniform feeding is shown in Fig. 5 compared to non-uniform feeding constructed pattern. The simulation results show that the non-uniform feeding is more accurate than the uniform feeding. The measured MSEs for both synthesized patterns using uniform feeding and non-uniform feeding are $\text{MSE}_{\text{uniform}} = -21.8728$ dB and $\text{MSE}_{\text{Non-uniform}} = -58.1917$ dB. However, the dynamic range ratio (DRR = maximin excitation/minimum excitation) of the non-uniform feeding is $\text{DRR}_{\text{Non-uniform}} = 486.8626$ which is much higher than the DRR of uniform feeding $\text{DRR}_{\text{uniform}} = 1$. The polar coordinates (r_m, ψ_m) and nodes energy transmissions (δ) for non-uniform feeding synthesized pattern of the selected $M = 40$ nodes are listed in Table 1 and Table 2 respectively.

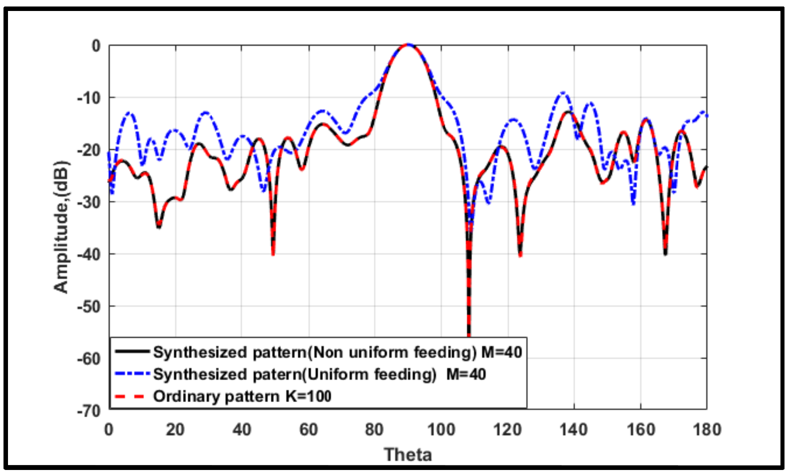

Figure 5. The synthesized patterns using uniform feeding and non-uniform feeding for $M = 40$ compared to the ordinary pattern using $K = 100$ for case (a) of nodes locations selection.

Table 1. The polar coordinates (r_m (meter), ψ_m (rad)) of $M = 40$ nodes for case (a) of nodes locations selection.

m	r_m	ψ_m	m	r_m	ψ_m	m	r_m	ψ_m	m	r_m	ψ_m
1	1.6623	−1.0320	11	3.2282	1.0389	21	3.6202	−0.7469	31	3.3799	1.5650
2	2.4147	−0.0311	12	5.5306	−0.1150	22	3.2508	0.3118	32	4.2293	0.5525
3	3.2585	0.9486	13	5.2048	−0.3414	23	5.8165	−1.1208	33	1.8923	0.2976
4	0.9686	−1.0528	14	3.5786	−1.4486	24	3.1532	−0.5616	34	3.8527	−1.0052
5	4.9705	−0.4815	15	4.6568	1.2970	25	5.8775	−1.5223	35	2.9829	−1.4586
6	4.1519	−1.2750	16	4.5582	0.3296	26	3.4128	−0.0490	36	3.3366	−1.1160
7	1.5929	0.9473	17	0.8593	−0.6731	27	4.4583	−0.5751	37	5.9536	1.4948
8	3.8800	−1.0706	18	1.9959	−1.1157	28	4.6277	1.3142	38	5.9885	−0.2514
9	4.1604	−1.1552	19	5.5364	−1.5486	29	5.6848	−1.5052	39	2.2670	−1.2193
10	2.8806	1.3480	20	3.3532	1.0484	30	4.3538	−1.4347	40	3.2155	0.2195

Table 2. The synthesized transmission energy δ_m(Amplitude$\angle$Phsae (rad)) for the selected $M = 40$ nodes for case (a) of nodes locations selection.

m	(δ_m)	m	(δ_m)	m	(δ_m)	m	(δ_m)
1	$262.3220\angle-1.1515$	11	$158.1997\angle1.6299$	21	$33.0702\angle2.3901$	31	$2.6809\angle3.1241$
2	$105.4153\angle-2.8957$	12	$34.5484\angle-0.3638$	22	$174.7939\angle-2.2557$	32	$53.9916\angle-2.9974$
3	$35.9868\angle-0.7638$	13	$95.2663\angle-0.7938$	23	$2.3295\angle1.7769$	33	$138.1213\angle2.0667$
4	$76.0121\angle1.6027$	14	$68.0386\angle-2.1460$	24	$106.8438\angle3.0544$	34	$237.0829\angle-0.7297$
5	$69.3376\angle1.0940$	15	$5.0982\angle2.5018$	25	$0.6415\angle2.8417$	35	$63.2607\angle0.0866$
6	$145.8333\angle2.7061$	16	$69.7554\angle1.5436$	26	$125.3512\angle-2.8022$	36	$202.7207\angle3.0371$
7	$48.3242\angle0.0637$	17	$89.5485\angle1.0910$	27	$20.7436\angle3.1147$	37	$0.5389\angle2.5784$
8	$34.2405\angle2.4940$	18	$195.1280\angle1.5260$	28	$3.6558\angle-0.6339$	38	$8.1697\angle1.0752$
9	$167.9948\angle0.2318$	19	$1.5061\angle-2.6606$	29	$2.2747\angle-1.5030$	39	$42.1376\angle-2.5619$
10	$11.3011\angle1.5838$	20	$140.7732\angle-1.4271$	30	$9.0836\angle0.2946$	40	$256.2589\angle-0.1369$

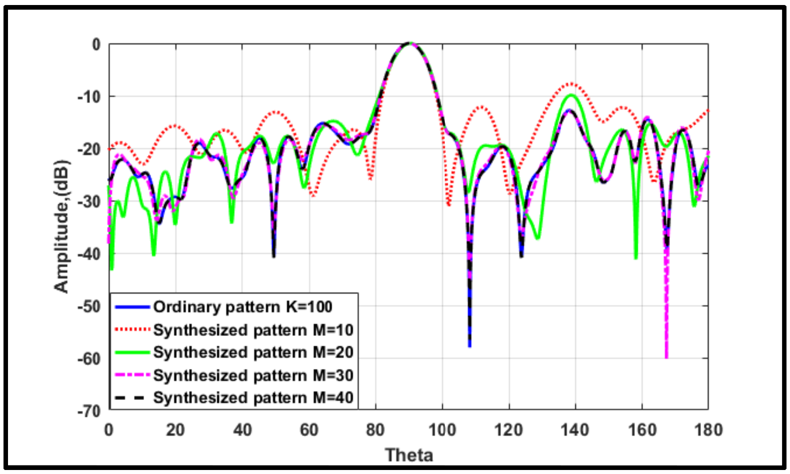

Figure 6. The synthesized patterns using non-uniform feeding for $M = 10$, 20, 30, and 40 and compared to the ordinary pattern using $K = 100$ for case (b) of nodes locations selection.

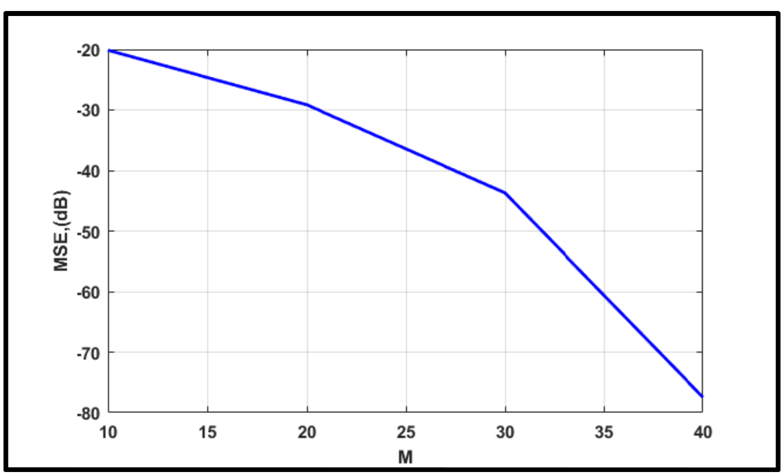

Figure 7. The MSE versus the number of nodes M for synthesized patterns using non-uniform feeding for case (b) of nodes locations selection.

Scenario (2): In this scenario, the desired M nodes are selected randomly from the original distributed K nodes with the same locations according to Eq. (11). These nodes are chosen after 1000 iterations for each M to select the minimum MSE. This way of selection is more efficient as it has more freedom for nodes selection. Fig. 6 shows the synthesized patterns using non-uniform feeding for $M = 10$, 20, 30, and 40. The synthesized pattern using $M = 40$ is extremely matched with the ordinary pattern using $K = 100$. Also, it provides the smallest MSE which equals $-77.4822\,\text{dB}$ while the synthesized patterns using $M = 10$, 20, 30 provide MSEs of $-20.1275\,\text{dB}$, $-29.1483\,\text{dB}$, and $-43.6963\,\text{dB}$, respectively. Fig. 7 shows the MSE versus the number of desired M nodes. Fig. 8 shows the distribution of $M = 40$ and $K = 100$ nodes. For $M = 40$, the synthesized patterns using uniform feeding and non-uniform feeding are shown in Fig. 9. The synthesized pattern using non-uniform feeding is more accurate than that using the uniform feeding because it provides much smaller MSE than the uniform feeding. The resultant MSEs are $\text{MSE}_{\text{uniform}} = -22.0687\,\text{dB}$ and $\text{MSE}_{\text{Non-uniform}} = -77.4822\,\text{dB}$. The polar coordinates (r_m, ψ_m) and the nodes energy transmissions (δ) for non-uniform feeding of the selected

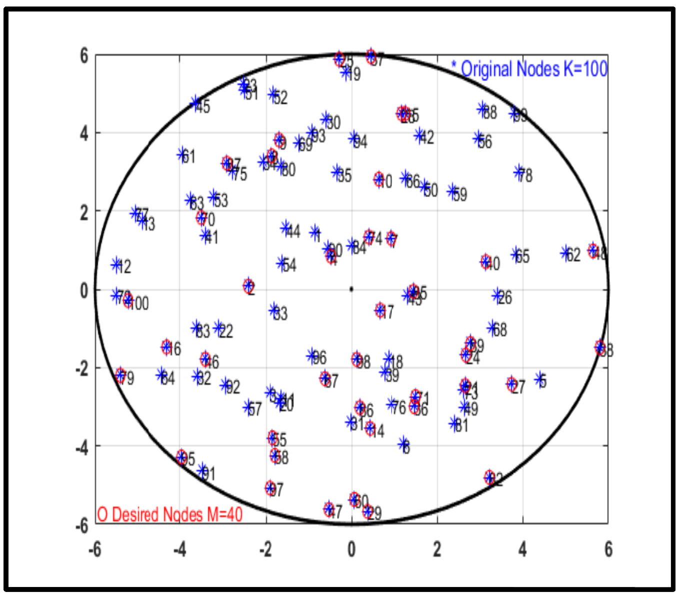

Figure 8. The distribution of $M = 40$ and $K = 100$ nodes over $R = 6\,\text{m}$ for case (b) of nodes locations selection.

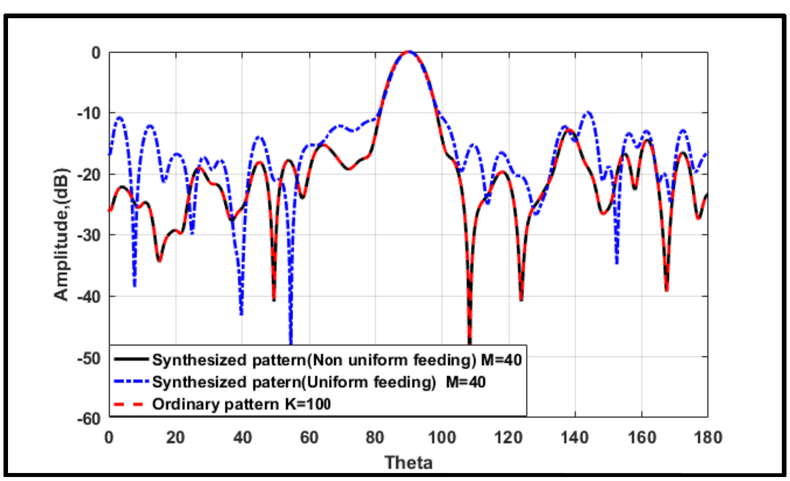

Figure 9. The synthesized pattern using uniform feeding and non-uniform feeding for $M = 40$ compared to the ordinary pattern using $K = 100$ for case (b) of nodes locations selection.

Table 3. The polar coordinates (r_m (meter), ψ_m (rad)) of $M = 40$ nodes for case (b) of nodes locations selection.

m	r_m	ψ_m	m	r_m	ψ_m	m	r_m	ψ_m	m	r_m	ψ_m
1	2.4147	−0.0311	11	3.3532	1.0484	21	3.8514	0.4831	31	5.8389	0.3864
2	0.9686	−1.0528	12	3.1532	−0.5616	22	5.6491	1.4774	32	5.7819	−0.9803
3	1.5929	0.9473	13	5.8775	−1.5223	23	5.7261	0.1712	33	1.4508	−0.0370
4	3.8800	−1.0706	14	4.4583	−0.5751	24	4.2135	1.1189	34	3.0278	−1.5068
5	4.1604	−1.1552	15	4.6277	1.3142	25	4.5990	1.1722	35	4.3341	−0.8355
6	2.8806	1.3480	16	5.6848	−1.5052	26	5.3635	−1.5580	36	3.1050	−0.4629
7	3.5786	−1.4486	17	3.3366	−1.1160	27	2.3674	1.3062	37	5.8375	0.8236
8	4.6568	1.2970	18	5.9536	1.4948	28	3.9537	−0.4806	38	5.4196	1.2121
9	4.5582	0.3296	19	5.9885	−0.2514	29	3.1243	−1.0695	39	1.7944	−1.5053
10	0.8593	−0.6731	20	3.2155	0.2195	30	1.3911	1.2766	40	5.2399	0.0546

Table 4. The Synthesized transmission energy δ_m(Amplitude$\angle$Phsae (rad)) for the desired $M = 40$ nodes for case (b) of nodes locations selection.

m	(δ_m)	m	(δ_m)	m	(δ_m)	m	(δ_m)
1	$2.7665\angle 1.1752$	11	$4.0877\angle 0.1595$	21	$2.8098\angle 2.7367$	31	$0.8407\angle -1.1206$
2	$6.3581\angle 2.4427$	12	$8.1414\angle -1.3680$	22	$0.5575\angle 0.5167$	32	$0.4969\angle -2.1611$
3	$2.3596\angle 1.0882$	13	$0.8938\angle -0.8928$	23	$0.7330\angle -1.7831$	33	$2.8648\angle -0.9969$
4	$7.6374\angle -2.3668$	14	$2.2772\angle -1.1634$	24	$2.8076\angle -1.2203$	34	$4.6646\angle 3.1290$
5	$4.2735\angle 0.9437$	15	$2.0778\angle 1.7820$	25	$4.8369\angle 2.5331$	35	$5.1230\angle -0.3074$
6	$3.2525\angle 2.4159$	16	$0.9283\angle 0.9600$	26	$1.1093\angle 2.9226$	36	$10.8126\angle 2.3484$
7	$4.4973\angle 0.7097$	17	$2.7239\angle 2.9244$	27	$4.4043\angle -1.5293$	37	$0.7934\angle 1.5150$
8	$2.6864\angle -0.6613$	18	$0.4066\angle -3.0152$	28	$8.0963\angle -2.2150$	38	$0.5819\angle 1.0147$
9	$1.6177\angle -1.4279$	19	$0.4502\angle -1.8029$	29	$5.4493\angle -0.2993$	39	$4.7957\angle 1.9994$
10	$5.0776\angle 0.8710$	20	$2.7027\angle -0.3668$	30	$4.2099\angle -0.9755$	40	$3.9129\angle 0.0849$

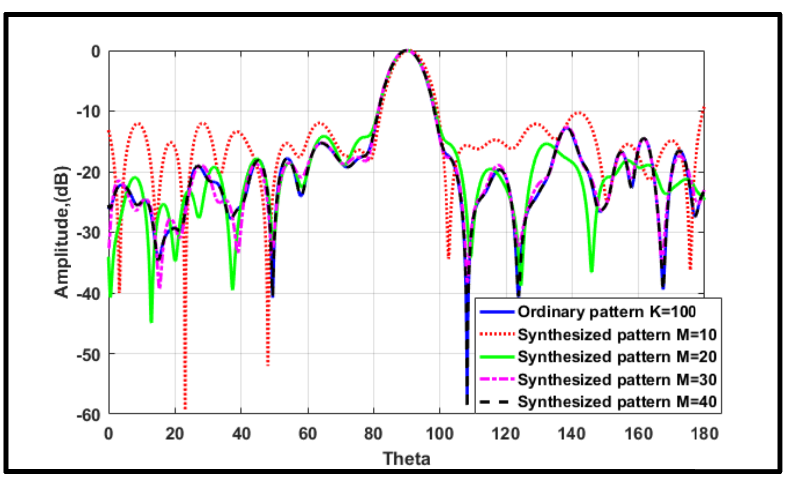

Figure 10. The synthesized patterns using non-uniform feeding for $M = 10$, 20, 30, and 40 compared to the ordinary pattern using $K = 100$ for case (c) of nodes locations selection.

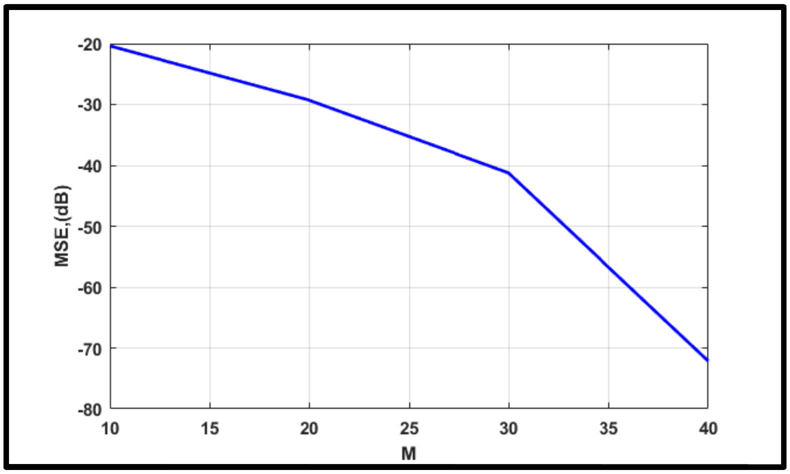

Figure 11. The MSE versus the number of nodes M for synthesized patterns using non-uniform feeding for case (c) of nodes locations selection.

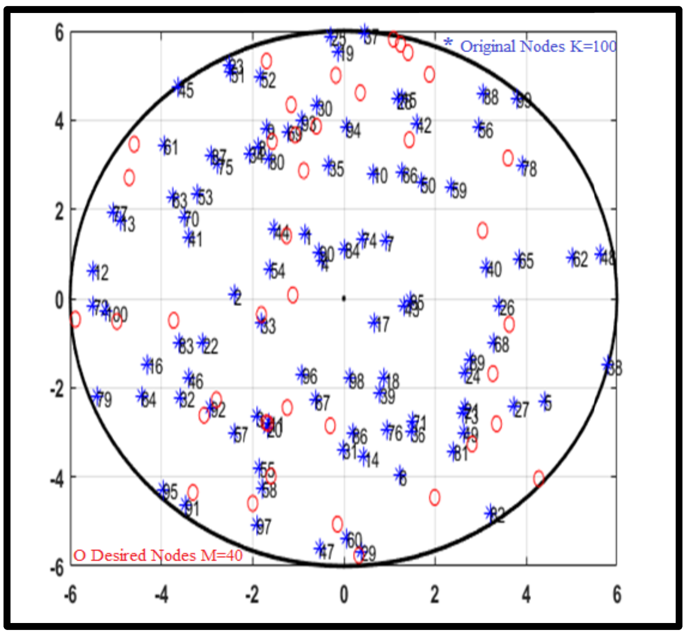

Figure 12. The distribution of $M = 40$ and $K = 100$ nodes over $R = 6\,\mathrm{m}$ for case (c) of nodes location selection.

$M = 40$ nodes are listed in Table 3 and Table 4, respectively. The dynamic range ratio of the non-uniform feeding is $\mathrm{DRR}_{\text{Non-uniform}} = 26.0687$ which is much smaller than the DRR of scenario (1).

Scenario (3): In this scenario, the desired M nodes are distributed randomly over the same disk with radius R with new locations according to Eq. (12). These nodes have polar coordinates which are completely different from the original distributed nodes. They are also selected after 1000 iterations for each M to achieve the minimum MSE. This way of selection increases the flexibility of the algorithm. However, it needs to build a new distributed antenna array. The synthesized patterns using non-uniform feeding for $M = 10$, 20, 30, and 40 are shown in Fig. 10. It is clear that the synthesized pattern using $M = 40$ highly agrees with the ordinary pattern using $K = 100$. Also, it provides the smallest MSE. For $M = 10$, 20, 30, and 40, the computed MSEs are $-20.5405\,\mathrm{dB}$, $-27.7516\,\mathrm{dB}$, $-41.2108\,\mathrm{dB}$, and $-72.1687\,\mathrm{dB}$, respectively. Fig. 11 shows the MSE versus different distributions of M nodes. The distribution of the desired $M = 40$ and the original $K = 100$ nodes are shown in Fig. 12.

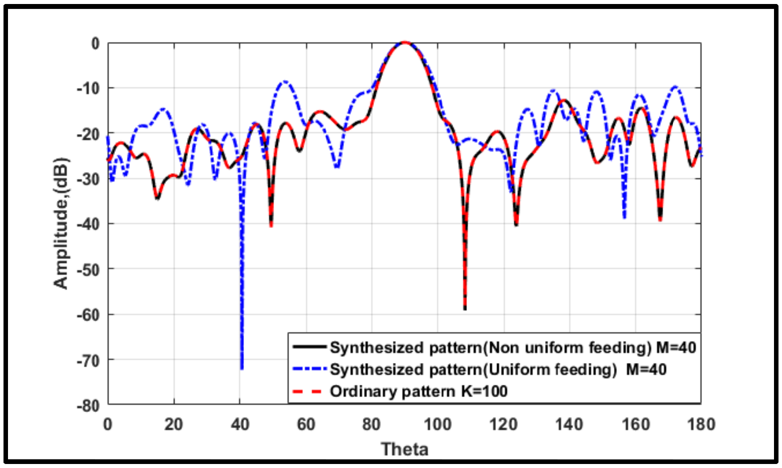

Figure 13. The synthesized pattern using uniform feeding and non-uniform feeding for $M = 40$ compared to the ordinary pattern using $K = 100$ for case (c) of nodes location selection.

Table 5. The polar coordinates $(r_m\,(\text{meter}), \psi_m\,(\text{rad}))$ of $M = 40$ nodes for case (c) of nodes location selection.

m	r_m	ψ_m	m	r_m	ψ_m	m	r_m	ψ_m	m	r_m	ψ_m
1	5.5871	-1.2635	11	4.2904	1.1903	21	1.8364	0.1977	31	3.6079	0.6810
2	2.9991	-1.2738	12	5.6888	1.3222	22	5.8806	-0.7568	32	4.4941	-1.3117
3	5.4340	-0.5225	13	4.7853	0.7183	23	5.0615	1.5429	33	1.8843	-0.8429
4	5.0081	-1.5357	14	4.6290	1.4933	24	5.8343	1.3579	34	5.9140	1.3868
5	1.1181	-0.0709	15	3.7699	0.1309	25	3.2543	1.0382	35	2.7431	1.1023
6	4.3753	-0.6974	16	4.0373	0.7056	26	5.0039	0.1025	36	5.3676	1.2118
7	3.4075	0.4637	17	5.9052	0.0791	27	2.8667	1.4665	37	4.3118	-0.8585
8	5.4686	0.9192	18	4.8894	-1.1488	28	3.6758	-0.1584	38	3.8336	1.1894
9	3.2606	1.0231	19	5.0069	1.1620	29	3.9118	-1.4161	39	3.8168	-1.2889
10	3.6802	-0.4750	20	3.8523	-1.1519	30	5.7690	-1.5141	40	5.7570	-0.6450

Table 6. The Synthesized transmission energy $\delta_m(\text{Amplitude}\angle\text{Phsae}\,(\text{rad}))$ for the desired $M = 40$ nodes for case (c) of nodes locations selection.

m	(δ_m)	m	(δ_m)	m	(δ_m)	m	(δ_m)
1	$1.3520\angle 2.3056$	11	$5.2840\angle-2.1406$	21	$3.4660\angle 1.0359$	31	$3.0359\angle-1.6119$
2	$0.8873\angle-1.6220$	12	$8.7834\angle-1.7293$	22	$0.5291\angle 0.4270$	32	$1.2742\angle-1.4033$
3	$2.8132\angle 2.5200$	13	$5.2144\angle 1.7181$	23	$2.0998\angle-0.6312$	33	$4.9328\angle-2.0188$
4	$0.8624\angle-1.2408$	14	$6.5647\angle-0.6998$	24	$6.1341\angle 3.0808$	34	$3.8969\angle 0.9217$
5	$1.8459\angle-0.4318$	15	$2.4482\angle-2.4817$	25	$4.7719\angle-1.8937$	35	$7.6181\angle 1.4411$
6	$3.9209\angle-1.8451$	16	$7.2257\angle-2.6289$	26	$4.5754\angle-2.6353$	36	$6.9596\angle 0.5232$
7	$2.7902\angle-0.7114$	17	$0.5749\angle-2.6039$	27	$8.3598\angle-2.1979$	37	$5.9609\angle 1.0346$
8	$3.9639\angle 1.7782$	18	$4.4536\angle 2.4528$	28	$2.2679\angle-0.0884$	38	$7.6838\angle 1.5336$
9	$6.7981\angle 0.0904$	19	$8.1881\angle 1.7672$	29	$2.9295\angle-2.4034$	39	$4.5267\angle 0.3053$
10	$4.3617\angle 0.3583$	20	$2.7512\angle-0.9780$	30	$1.2094\angle-0.9690$	40	$1.1018\angle 1.7589$

For $M = 40$, the synthesized patterns using uniform feeding and non-uniform feeding are shown in Fig. 13. The synthesized pattern using non-uniform feeding coincides with the ordinary pattern using $K = 100$. However, the synthesized pattern using uniform feeding has major variations compared to the ordinary pattern. It also provides $\text{MSE}_{\text{uniform}} = -21.1656\,\text{dB}$ which is much higher than the MSE of the synthesized pattern using non-uniform feeding which equals $\text{MSE}_{\text{Non-uniform}} = -72.1687\,\text{dB}$. The polar coordinates (r_m, ψ_m) and the nodes energy transmissions (δ) for non-uniform feeding of the selected $M = 40$ nodes are listed in Table 5 and Table 6, respectively. The dynamic range ratio of the non-uniform feeding is $\text{DRR}_{\text{Non-uniform}} = 16.601$ which is much smaller than the DRR of scenario (1) and scenario (2).

The simulation results of the three scenarios are summarized in brief in Table 7 which contains the computed MSEs, and DRRs of the synthesized arrays at $M = 40$ nodes for the three cases of nodes locations selection applying non-uniform and uniform feeding.

Table 7. The computed MSEs and DRRs of the synthesized arrays using $M = 40$ nodes for the three cases of nodes locations selection applying non-uniform and uniform feeding.

Feeding Technique	**Scenario (1)**		**Scenario (2)**		**Scenario (3)**	
	MSE	**DRR**	**MSE**	**DRR**	**MSE**	**DRR**
Non-uniform	−58.1917 dB	486.8626	−77.4822 dB	26.0687	−72.1687 dB	16.601
Uniform	−21.8728 dB	1	−22.0687 dB	1	−21.1656 dB	1

4. CONCLUSION

In this paper, an efficient distributed array synthesis algorithm is proposed to reduce the number of distributed nodes in wireless sensor networks. It controls the number of nodes, node locations, and the excitation of each node. The desired patterns are synthesized using non-uniform and uniform excitations. The simulation results reveal that all the proposed nodes locations selection schemes have the ability to generate a synthesized pattern which completely agrees with the ordinary pattern at a sufficient number of nodes M. In terms of MSE and DRR, the second and third scenarios are recommended for array synthesis as they provide the lowest values for MSE and DRR. Also, they provide more freedom for nodes distribution over the intended area. In future work, the capabilities of the algorithm can be extended to synthesize non-coplanar distributed antenna arrays taking into account real antenna elements instead of isotropic elements assumption.

REFERENCES

1. Huang, J., P. Wang, and Q. Wan, "Collaborative beamforming for wireless sensor networks with arbitrary distributed sensors," *IEEE Communications Letters*, Vol. 16, No. 7, 1118–1120, 2012.
2. Valenzuela-Valdes, J., F. Luna, R. Luque-Baena, and P. Padilla, "Saving energy in WSNs with beamforming," *Proc. IEEE 3rd Int. Conf.*, 255–260, Cloud Netw., (CloudNet), 2014.
3. Jung, H. and I.-H. Lee, "Analog cooperative beamforming with spherically-bound random arrays for physical-layer secure communications," *IEEE Communications Letters*, Vol. 22, No. 3, 546–549, 2018.
4. Ma, N. N., K. Buchanan, J. Jensen, and G. Huff, "Distributed beamforming from triangular planar random antenna arrays," *MILCOM 2015 — 2015 IEEE Military Communications Conference*, 553–558, 2015.
5. Bhattacharyya, A. K., *Phased Array Antennas: Floquet Analysis, Synthesis, BFNs and Active Array Systems*, John Wiley & Sons, 2006.
6. Madhow, U., D. R. Brown, S. Dasgupta, and R. Mudumbai, "Distributed massive MIMO: Algorithms, architectures and concept systems," 1–7, *2014 Information Theory and Applications Workshop (ITA)*, 2014.

7. Zhang, X., D. Wang, L. Bai, and C. Chen, "Collaborative relay beamforming based on minimum power for M2M devices in multicell systems," *International Journal of Distributed Sensor Networks*, Vol. 9, No. 12, 293565, 2013.
8. Ochiai, H., P. Mitran, H. V. Poor, and V. Tarokh, "Collaborative beamforming for distributed wireless ad hoc sensor networks," *IEEE Transactions on Signal Processing*, Vol. 53, No. 11, 4110–4124, 2005.
9. Sun, G., Y. Liu, A. Wang, J. Zhang, X. Zhou, and Z. Liu, "Sidelobe control by node selection algorithm based on virtual linear array for collaborative beamforming in WSNs," *Wireless Personal Communications*, Vol. 90, No. 3, 1443–1462, 2016.
10. Liang, S., T. Feng, G. Sun, J. Zhang, and H. Zhang, "Transmission power optimization for reducing sidelobe via bat-chicken swarm optimization in distributed collaborative beamforming," *2016 2nd IEEE International Conference on Computer and Communications (ICCC)*, 2164–2168, 2016.
11. Jayaprakasam, S., S. K. A. Rahim, and C. Y. Leow, "Distributed and collaborative beamforming in wireless sensor networks: Classifications, trends, and research directions," *IEEE Communications Surveys & Tutorials*, Vol. 19, No. 4, 2092–2116, 2017.
12. Jayaprakasam, S., S. K. B. A. Rahim, and C. Y. Leow, "A pareto elite selection genetic algorithm for random antenna array beamforming with low sidelobe level," *Progress In Electromagnetics Research B*, Vol. 51, 407–425, 2013.
13. Liu, Y., Z. Nie, and Q. H. Liu, "Reducing the number of elements in a linear antenna array by the matrix pencil method," *IEEE Trans. Antennas Propag.*, Vol. 56, No. 9, 2955–2962, Sep. 2008.
14. Liu, Y., Q. H. Liu, and Z. Nie, "Reducing the number of elements in the synthesis of shaped-beam patterns by the forward-backward matrix pencil method," *IEEE Trans. Antennas Propag.*, Vol. 58, No. 2, 604–608, Nov. 2010.
15. Hussein, A., H. Abdullah, A. Salem, S. Khamis, and M. Nasr, "Optimum design of linear antenna arrays using a hybrid MoM/GA algorithm," *IEEE Antennas and Wireless Propagation Letters*, Vol. 10, 1232–1235, 2011.
16. Isernia, T. and A. F. Morabito, "Mask-constrained power synthesis of linear arrays with even excitations," *IEEE Trans. Antennas Propag.*, Vol. 64, No. 7, 3212–3217, 2016.